Bulletin of Electrical Engineering and Informatics
Vol. 15, No. 1, February 2026, pp. 637∼647
ISSN: 2302-9285, DOI: 10.11591/eei.v15i1.9438

Power-LSTM for smart greenhouse: a novel deep learning approach to temperature prediction in a Mexican case study

Salma Ait Oussous, Dauris Lail Madama, Rachid El Bouayadi, Aouatif Amine
Advanced Systems Engineering (ISA) Laboratory, National School of Applied Sciences, Ibn Tofail University, Kenitra, Morocco

Article Info

Article history:

Received Oct 14, 2024
Revised Sep 9, 2025
Accepted Dec 6, 2025

Keywords:

Artificial neural network
Deep learning
Greenhouse temperature
LSTM-artificial neural network
LSTM-recurrent neural network
Power-long short-term memory

ABSTRACT

This paper addresses the challenge of predicting internal temperature in greenhouse environments, a critical aspect of optimizing crop growth and ensuring resource efficiency. While machine learning (ML) techniques have been widely applied to predict greenhouse climates, deep learning (DL) methods offer the potential to capture more complex relationships within the data. In this study, we present a comprehensive evaluation of ML and DL models, along with our proposed power-long short-term memory (PLSTM) model, to predict the internal temperature of a greenhouse using a database from Mexico. We compared traditional ML models such as linear regression (LR) and extreme gradient boosting (XGBoost) with DL architectures like gated recurrent unit (GRU), artificial neural networks (ANN), hybrid LSTM-ANN and LSTM-RNN architectures. Our proposed PLSTM model outperformed both ML and DL models, achieving the R^2 score of 0.9710, and root mean square error (RMSE) equal to 0.1710, highlighting its superior ability to predict complex time-series data.

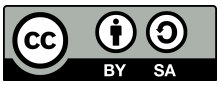

Corresponding Author:

Salma Ait Oussous
Advanced Systems Engineering (ISA) Laboratory, National School of Applied Sciences
Ibn Tofail University
Kenitra, Morocco
Email: salma.aitoussous@uit.ac.ma

1. INTRODUCTION

The increasing demand for sustainable agriculture has created a need for more advanced greenhouse management strategies. These strategies aim to maximize crop yields while minimizing resource consumption [1]. An important aspect of greenhouse control is accurately predicting internal temperature, as it directly impacts plant growth and energy usage [2].

In our previous study [3], we explored the use of machine learning (ML) models such as linear regression (LR) and extreme gradient boost (XGBoost) to forecast greenhouse temperature using data from two different greenhouse environments. We also investigated the correlation between the parameters: external temperature, solar irradiance, internal humidity, external humidity, and dew point. While these models showed reasonable accuracy, they may struggle to handle the complexities of temporal climate data.

In recent years, deep learning (DL) models have shown significant potential in handling time-series data, thanks to their ability to capture intricate relationships over time [4]. Architectures like recurrent neural networks (RNNs), long short-term memory (LSTM), and gated recurrent units (GRU) are well-suited for such tasks. These models are designed to address the vanishing gradient problem and can effectively model long-term dependencies [5]. Additionally, hybrid architectures like LSTM-ANN and LSTM-RNN offer a flexible

approach by combining the strengths of both recurrent and feedforward models to improve predictive capabilities [6].

This study aims to answer the following research question: Can DL models, particularly the proposed Power-LSTM (PLSTM), significantly improve the accuracy of greenhouse temperature prediction compared to traditional ML models and standard DL architectures? To address this question, we extend our previous work by comparing the performance of several DL models—ANN, GRU, LSTM-ANN, LSTM-RNN—and our proposed PLSTM model, against LR and XGBoost. The models are evaluated using ten different input feature combinations based on a comprehensive greenhouse database collected in Mexico. Performance is assessed using metrics such as the coefficient of determination (R^2) and root mean square error (RMSE).

This research makes a significant contribution to the advancement of intelligent greenhouse systems by demonstrating how DL can enhance the precision and reliability of climate control strategies. Accurate temperature forecasting not only optimizes plant growth conditions but also reduces unnecessary energy consumption, supporting more sustainable and cost-effective operations. A key novelty of this study lies in the introduction of the PLSTM model, specifically designed to capture complex temporal dependencies within greenhouse data. Additionally, the evaluation of various DL models across ten diverse input combinations offers a robust comparison of predictive capabilities.

Moreover, this study is embedded within a larger initiative that includes the realization of a physical greenhouse system, sensor-based data collection, and the deployment of a comprehensive IoT framework for analysis and control. Together, these efforts reflect the transition from theoretical modeling to applied smart agriculture solutions, making the research both technically sound and practically relevant.

This paper is structured as follows: section 1, introduces the main objective of the work. Section 2, outlines the proposed method and implemented architecture. Section 3, presents the results and discusses the performance of the tested models. Finally, section 4 offers the conclusion and future perspectives.

2. METHOD

To achieve the goal of this study, we used a greenhouse database from South Mezquitera, Juchipila, Zacatecas, Mexico, spanning from July 12, 2020 to June 24, 2021. This database was used in our previous research [3], alongside a database from Spain, where we compared the performance of ML models with the PLSTM for temperature greenhouse prediction. To ensure continuity and build upon previous findings, we apply DL methods in this study using the Mexican database.

Despite efforts to find other sources, we encountered a notable lack of accessible, high-quality greenhouse databases suitable for our experiments. Consequently, this database was selected due to its completeness and relevance. Furthermore, the choice is supported by agronomic and climatic similarities between Morocco and regions such as Mexico and Spain. For instance, Zacatecas in Mexico and semi-arid regions of Morocco exhibit comparable climatic conditions characterized by high solar radiation, limited rainfall, and warm temperatures that affect greenhouse environments in similar ways. These parallels have been underscored in several studies. For example, [7] highlight that both Morocco and Spain share Mediterranean climate characteristics, common crop varieties, and similar agricultural practices, supporting the validity of cross-regional comparisons. Additionally, [8] describes Morocco as "North Africa's California," noting its Mediterranean climate, fertile soils, and horticultural potential, which closely mirror those found in parts of Spain and Mexico. Finally, the use of this database serves as a temporary alternative while awaiting the availability of data from our own experimental greenhouse currently under development in Morocco. The selected database includes internal temperature (Ti) in °C, external temperature (To) in °C, internal humidity (Hi) in %, external humidity (Ho) in %, solar irradiance (Rs) in W/m², and internal dew point (Di) in %.

The main objective of this paper is to develop and evaluate DL models for the accurate prediction of internal greenhouse temperature. While the impact of predictive accuracy on broader agricultural factors such as energy consumption, crop yield, and operational efficiency is undoubtedly important, these aspects are outside the scope of the present study. They are being investigated in parallel by another research team within the same project, as part of a complementary effort focused on the optimization of greenhouse resource management.

In this study, we conducted experiments using three input features and one output (Ti), testing ten different combinations to assess their influence on prediction performance. These combinations are summarized in Table 1.

Table 1. Sequence of input-output variables (as presented in [3])

Combination number	1	2	3	4	5	6	7	8	9	10
Output	Ti									
Inputs	Hi-Di-To	Hi-Ho-To	Hi-To-Rs	Di-Rs-To	Ho-To-Rs	Hi-Di-Rs	Hi-Di-Ho	Hi-Rs-Ho	Di-Rs-Ho	Di-Ho-To

To further understand the relationships between the input variables and the target variable (Ti), we employed the Spearman Rank Coefficient. This measure is suitable for evaluating the strength and direction of relationships between variables, even when the data is not normally distributed. By calculating the Spearman Rank Coefficient for each pair of variables, we identified significant correlations and explored how changes in one variable relate to changes in another. The formula to calculate Spearman's rank correlation coefficient is presented (1):

$$\rho = 1 - \frac{6 \sum d_i^2}{n(n^2 - 1)} \tag{1}$$

where: d_i is the variance in ranks between the paired observations and the predicted value and n signifies the total count of observations [9].

To visualize these relationships and gain a comprehensive understanding of the interdependencies between the input variables, we created heat maps. Heatmaps are a graphical representation of data where each value is represented by a color, making it easy to identify patterns and trends [10]. In our analysis, the heatmap displayed the Spearman Rank Coefficient values between each pair of variables, with different colors representing varying degrees of correlation. This visual representation provided valuable insights into the relative importance of different input variables in predicting internal temperature and helped us identify potential redundancies or dependencies among the features. The heatmap for the Mexico Greenhouse Database, presented in Figure 1, reveals several key insights:

- Higher humidity (Hi, Ho) levels are associated with a decrease in internal temperature (Ti).
- An increase in solar radiation (Rs) corresponds to a rise in internal temperature (Ti).
- A rise in the dew point (Di) is linked to an increase in internal temperature (Ti).
- Elevated internal temperature (Ti) is connected to higher external temperature (To).

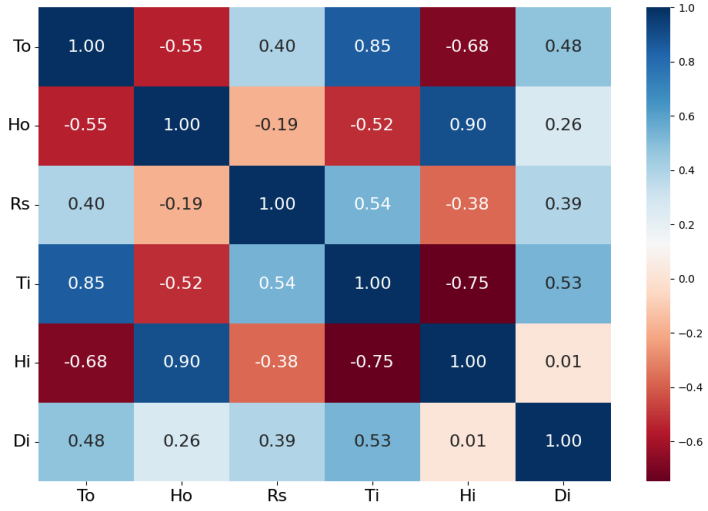

Figure 1. The Spearman correlation heatmap of Mexico greenhouse database

2.1. Model experiments

In our experiments, we selected a diverse DL models—GRU, ANN, LSTM-ANN, and LSTM-RNN—to explore their effectiveness in predicting greenhouse internal temperature. These models were chosen based on their unique strengths in handling time-series data and their ability to capture complex patterns inherent in greenhouse conditions. To provide a comprehensive comparison, we also included two ML models: LR and

XGBoost, which were successfully implemented in our previous work. In addition, we re-evaluated the performance of our proposed PLSTM model, which was introduced in earlier research as an advanced solution for this prediction task [3].

We split the Mexico greenhouse database into training, testing, and validation subsets to ensure robust model evaluation. Each model was trained and optimized through a hyperparameter tuning process, where we utilized Bayesian optimization to efficiently adjust the models' parameters. This approach was particularly advantageous in optimizing the objective functions, which require significant computational resources and time to evaluate, ensuring that each model was fine-tuned for maximum performance [11].

2.1.1. Gated recurrent unit model

GRU is a variant of the RNN that simplifies the structure of LSTM [12]. It uses gating units to control the flow of information and has two gates: the update gate (2) and the reset gate (3). In (4) represents candidate activation and final memory at current time step with (5).

$$z_t = \sigma(W_z \cdot x_t + U_z \cdot h_{t-1} + b_z) \tag{2}$$

$$r_t = \sigma(W_r \cdot x_t + U_r \cdot h_{t-1} + b_r) \tag{3}$$

$$\tilde{h}_t = \tanh(W_h \cdot x_t + r_t \odot (U_h \cdot h_{t-1}) + b_h) \tag{4}$$

$$h_t = (1 - z_t) \odot h_{t-1} + z_t \odot \tilde{h}_t \tag{5}$$

where: x_t is the input at time step, t, h_t is the hidden state at time step t, h_{t-1} is the hidden state at the previous time step, $\tilde{h}_t$ is the candidate hidden state, W_z, W_r, W_h are the weight matrices corresponding to the update gate, reset gate, and candidate hidden state, U_z, U_r, U_h are the recurrent weight matrices, b_z, b_r, b_h are the bias vectors, σ denotes the sigmoid activation function, $\tanh$ denotes the hyperbolic tangent activation function, and $\odot$ denotes element-wise multiplication [13].

2.1.2. Artificial neural network model

ANN are highly effective tools commonly used for recognizing and modeling complex systems, like those present in structural dynamics [14]. It functions like the human brain and neural systems, ANNs are created to imitate the capacity to learn and process information [15]. They consist of an extensive network of computer neurons, the fundamental units, connected by links that transmit signals in a single direction, similar to synapses in the human brain [16]. In an ANNs, each processing unit sends its signal through a single output, which can branch into several connections. These neurons work together to perform calculations much faster than traditional computers.

The model is constructed with three distinct layers: the input layer, the hidden layer, and the output layer [17]. The input layer comprises nodes, with one dedicated to each independent variable, while the output layer consists of a single node. The number of hidden layers can vary, with the complexity and size of the data determining whether a single hidden layer or multiple hidden layers are used. Neurons within each layer are connected to neurons in adjacent layers through weighted connections, and each neuron applies an activation function to its input [18]. During training, the model adjusts the weights and biases of these connections to minimize the error between predicted and actual results. In (6) describes the model calculation:

$$a = \sigma\left(\sum_{i=1}^{n} w_i x_i + b\right) \tag{6}$$

where: σ is the activation function, w_i are the weights associated with the input features, x_i are the input features and b is the bias term. While Table 2 provides details of the hyperparameters used in the ANN model [19].

Table 2. Optimal hyperparameters used for: GRU, ANN, LSTM-ANN, and LSTM-RNN

Parameter	Value				Description
	GRU	ANN	LSTM-ANN	LSTM-RNN	
Input size	3	3	3	3	Number of input features
Hidden size	250	250	250	250	Number of units in the hidden layer
Epochs	300	300	300	300	Number of complete passes through the training database
Batch size	620	620	620	620	Number of samples processed before updating the model
Learning rate	0.005	0.005	0.005	0.005	Rate at which the model's weights are updated
Optimizer	Adam	Adam	Adam	Adam	Optimization algorithm used for training
Dropout rate	-	0.2	-	0.2	Fraction of input units to drop during training
Activation function	-	ReLU	-	ReLU	Activation function used in the hidden layers
Gradient threshold	-	-	0.8	-	Maximum gradient value allowed during training
Drop factor	-	-	125	-	Factor by which learning rate is reduced after each epoch

2.1.3. Long short-term memory-recurrent neural network model

LSTM-RNN algorithm is a model which combines LSTM and RNN architecture. It memorizes well the historical data in sequential data and preserves information about the previous one [20].

Figure 2 visualizes the design of LSTM architecture. It uses a three-set of gates to control the sequence flow of data. The first is the forget gate (F_t), which decides which information to throw away from the cell state. It takes the previous hidden layer $H_t - 1$ and the current input X_t and produces a vector of values between 0 (completely get rid of this) and 1 (completely keep this) for each component of the cell state. The input gate (I_t) determines which new data should be stored in long-term memory, considering both the current input X_t and the previous hidden state $H_t - 1$. It uses the tanh activation function to combine these inputs and generate potential data. The sigmoid activation function then decides which elements of these candidate data are worth retaining, resulting in updated long-term memory. The output gate (O_t) defines the actual output of the cell. It takes into account the cell state and the input, producing an output that is filtered based on both the cell state and the internal state of the LSTM cell [21].

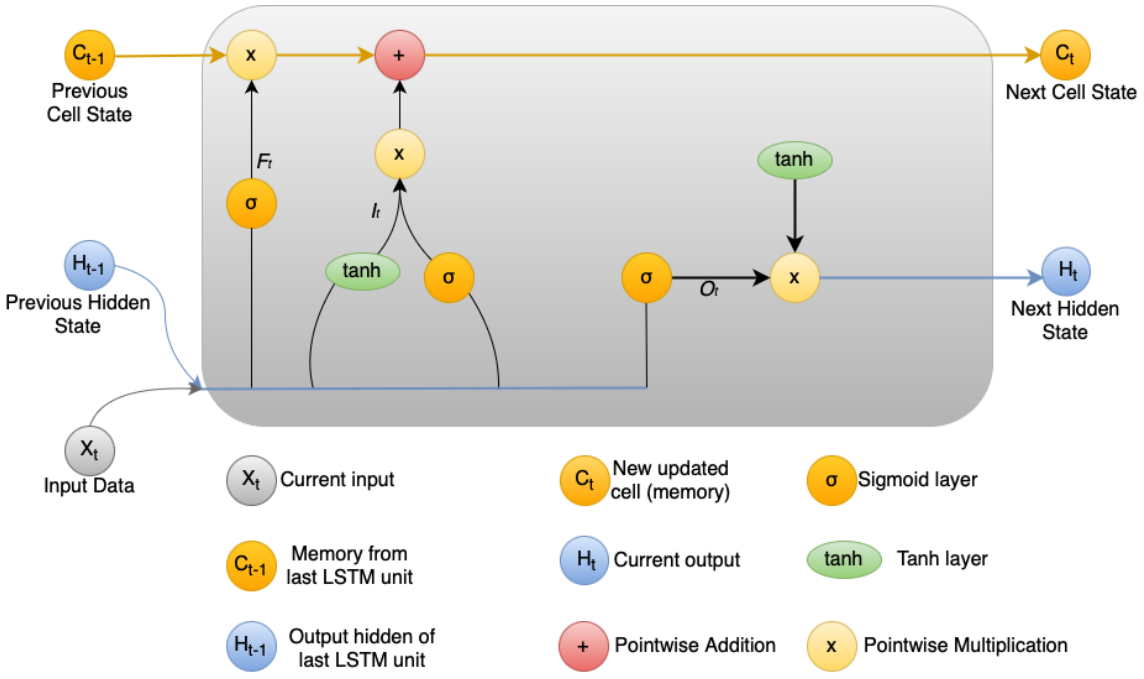

Figure 2. LSTM-RNN model architecture

2.1.4. Long short-term memory-artificial neural network model

The LSTM-ANN architecture is an innovative fusion that combines the characteristics of LSTM with those of standard ANNs. This combination aims to leverage the ability of LSTMs to process data sequences and combine it with the effectiveness of ANNs in areas such as classification, regression, and other forms of data analysis [22]. To understand how past events influence present ones, we take previous results into account

when training our model. However, we only focus on the most recent data to predict what will happen next. After gathering a comprehensive data set that reflects every conceivable operational condition, the next step is to train our neural network with this information [23]. By using multiple layers of LSTM, where each layer uses the previous layer's hidden units as input, we can model complex processes and discover hidden information in a hierarchical structure. This fusion of LSTM and ANN is ideal for processing data that vary or do not vary with time. LSTM networks process current data considering previous information and state internals to produce new outputs and states [24]. On the other hand, ANNs use a network of interconnected units in their hidden layer to process data, relying on nonlinear activation functions like the sigmoid and the hyperbolic tangent, thus facilitating complex operations like element-by-element multiplication and addition. The model was trained via DL with TensorFlow. Several optimizers were tried, including RMSProp, SGD, and Adam; nevertheless, the Adam optimizer was selected for this study. The optimal configuration was established after several attempts by adjusting the network hyperparameters such as the number of layers and neurons, the type of activation function, the batch size and the dropout rate. A detailed overview of the optimal hyperparameters used for each mentioned model is included in Table 2.

2.2. Experimental setup and model evaluation

For our experiments, we used Python 3.7 as programming language, with Keras 2.3.1, a TensorFlow-built high-level neural network API, for model development and training. Google Colab was used as the primary development environment due to its cloud-based computing capabilities and GPU acceleration, which significantly enhanced the efficiency of the training process. The performance of the models was evaluated using several metrics to ensure the reliability and accuracy of predictions. Specifically, we employed the (R^2), given its ability to measure how well the predicted values match the actual data and RMSE to further analyze the predictive accuracy and model performance [25].

3. RESULTS AND DISCUSSION

In our previous work [3], we studied the predictive capabilities of ML models, specifically LR and XGBoost, to forecast greenhouse temperature. We chose LR for its simplicity in modeling linear relationships and XGBoost's efficiency in handling non-linear relationships through gradient boosting [26]. However, as the data became more complex and voluminous, these models showed significant limitations. To address these challenges, we transitioned to DL techniques, including ANN, and proposed our novel LSTM-based model, named PLSTM, which had promising results.

In this study, our goal is to compare the performance of several DL models with ML models. To achieve this, we forecast four DL models: GRU, ANN, LSTM-ANN, and LSTM-RNN as seen in Table 3 and compared them with the ML models studied in our previous work (refer to Table 2) using the Mexico greenhouse database [3]. To make this comparison, we evaluated the performance of these models using the R^2 and RMSE metrics, considering ten different combinations of input variables.

Table 3. Comparison of DL models using ten combinations for Mexico greenhouse database

Metrics	R^2				RMSE			
Input-models	GRU	ANN	LSTM-ANN	LSTM-RNN	GRU	ANN	LSTM-ANN	LSTM-RNN
Hi-Di-To	**0.9547**	**0.9580**	**0.9690**	**0.9620**	**3.1903**	**0.2060**	**0.1760**	**2.9234**
Hi-Ho-To	0.9303	0.9300	0.9340	0.9307	3.9585	0.2650	0.2570	3.9465
Hi-To-Rs	0.9277	0.9340	0.9390	0.9361	4.0324	0.2570	0.2480	3.7903
Di-Rs-To	0.9063	0.9140	0.9190	0.9182	4.5900	0.2950	0.2860	4.2882
Ho-To-Rs	0.8993	0.9120	0.9160	0.9114	4.7581	0.2980	0.2920	4.6240
Hi-Di-Rs	0.9476	0.9510	0.9560	0.9526	3.4248	0.2230	0.9210	3.2626
Hi-Di-Ho	0.9415	0.9370	0.9460	0.9422	3.6279	0.2520	0.2340	3.6058
Hi-Rs-Ho	0.8781	0.8850	0.8860	0.8841	5.2367	0.3410	0.3400	5.1060
Di-Rs-Ho	0.9016	0.9160	0.9210	0.9142	4.7043	0.2920	0.2830	4.3933
Di-Ho-To	0.9115	0.9190	0.8240	0.9160	4.4609	0.2860	0.4210	4.3457

Firstly, the GRU model exhibited the best results with the Hi-Di-To combination, showing the highest R^2 value of 0.9547 and the lowest RMSE of 3.1903. Meanwhile, the Hi-Rs-Ho combination showed the lowest performance with R^2=0.8781 and RMSE=5.2367. For the ANN model, the Hi-Di-To combination had the highest R^2 value of 0.9580 and the lowest RMSE of 0.2060. On the other hand, Hi-Rs-Ho had the lowest

performance with R^2=0.8850 and RMSE=0.3410. In the case of the LSTM-ANN model, the Hi-Di-To combination registered the highest R^2 value of 0.9690 and the lowest RMSE of 0.1760. Di-Ho-To's combination had the lowest performance with R^2=0.8240 and RMSE=0.4210. In the LSTM-RNN model, the Hi-Di-To combination had the highest R^2 value of 0.9620 with a reasonable RMSE of 2.9234. In contrast, the Hi-Rs-Ho combination had the lowest performance with R^2=0.8841 and RMSE=5.1060.

The plots presented in Figure 3 visualize the performance of different predictive models in greenhouse temperature forecasting based on two key performance metrics: R^2 and RMSE. The x-axis lists the various models, providing a clear basis for comparison. The left y-axis displays R^2 values, which indicate the proportion of variance explained by each model. Higher values (closer to 1) signify better predictive accuracy. The right y-axis presents RMSE values, which quantify the average error between predicted and actual values, with lower values indicating better model performance. In this analysis PLSTM achieved the highest R^2 value of 0.9710, indicating excellent predictive capability, also boasts the lowest RMSE of 0.1710, demonstrating its precision in temperature predictions.

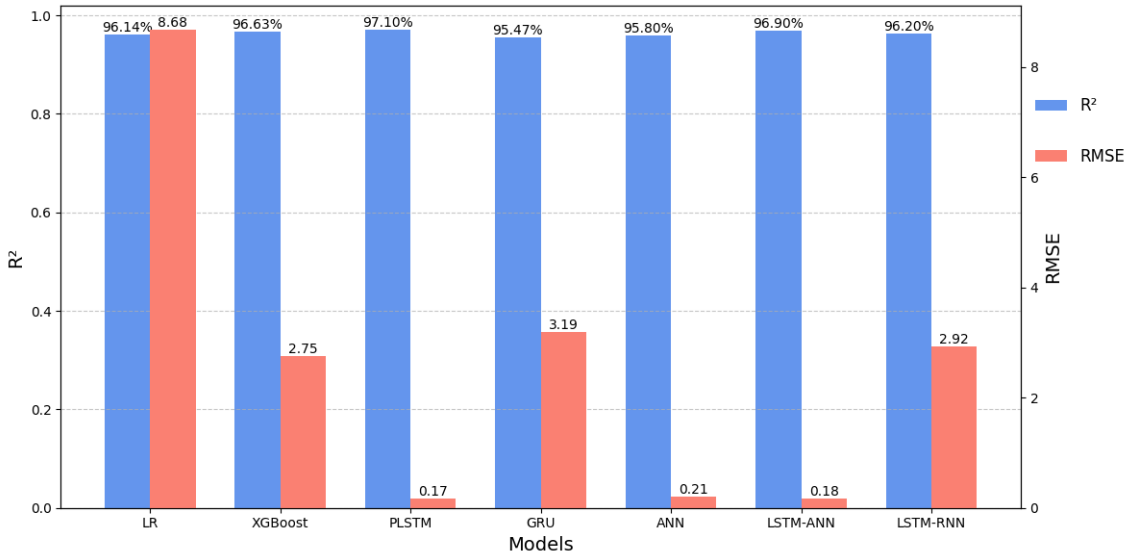

Figure 3. RMSE and R^2 estimations for different DL algorithms using with the best combination Hi-Di-To

Secondly, we compared the performance of these models using scatter plots to provide a clear representation of the predicted values of each model against the actual values. Figure 4 presents the scatter plot. The plot in Figure 4(a) compares real vs. predicted temperature values using ML models, while the plot in Figure 4(b) shows real vs. predicted temperature with DL models.

Starting with Figure 4(a), the LR, XGBoost, and PLSTM models are compared. The LR model, being a simpler ML model, shows that most of the points lie farther from the diagonal line, indicating significant deviations. This suggests that LR struggles with capturing the nonlinearities present in the data. The XGBoost model exhibits a better alignment with the diagonal compared to LR, indicating improved predictive accuracy. However, there are still some outliers. On the other hand, the proposed PLSTM model stands out as the most accurate, with a substantial concentration of points clustered closely around the diagonal line. This alignment suggests that the model effectively captures the underlying patterns in the data, resulting in highly accurate predictions across the temperature spectrum. For Figure 4(b), the scatter plot analyzes the DL models: ANN, GRU, LSTM-ANN, LSTM-RNN, and PLSTM. The scatter points for the ANN model display considerable dispersion from the diagonal line. GRU, LSTM-ANN, and LSTM-RNN models exhibit improvements over ANN, with more points clustering near the diagonal. While these models demonstrate a better understanding of the data, they still display occasional deviations. On the other hand, PLSTM is consistent with the first plot and again shows exemplary performance, with most points closely aligned with the diagonal line. This reinforces the model's ability to achieve accurate predictions and effectively adapt to variations in greenhouse temperature.

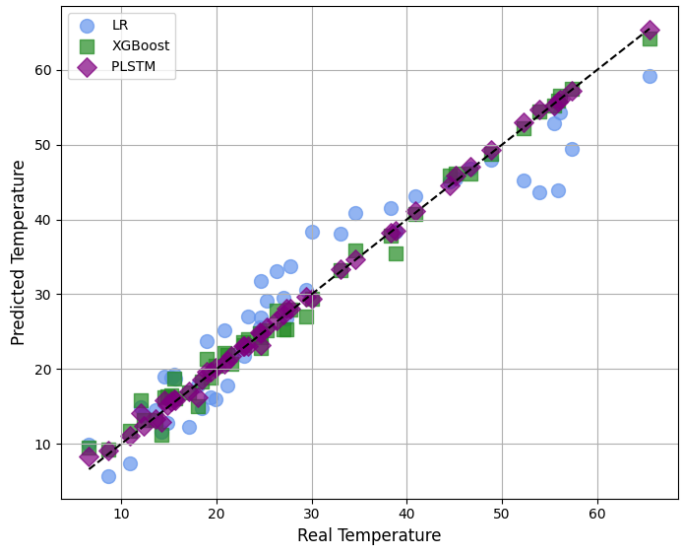

(a)

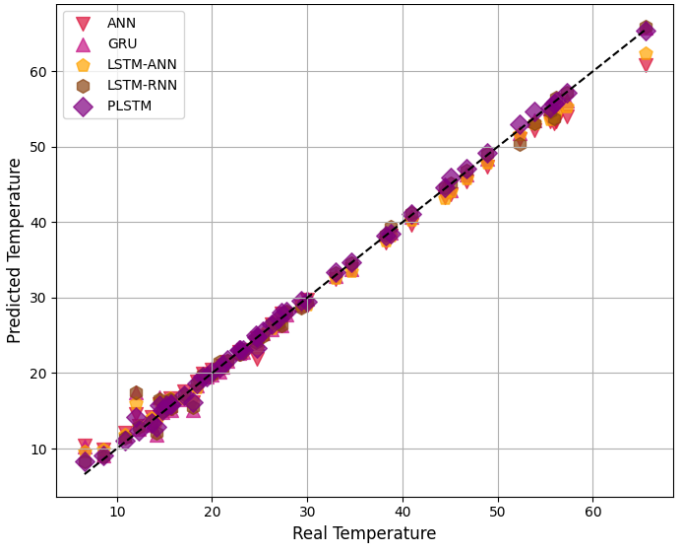

(b)

Figure 4. Scatter plot comparison: real vs predicted temperature values with; (a) ML and (b) DL

4. CONCLUSION

In summary, we compared various ML and DL models for predicting greenhouse temperature, with a particular focus on the performance of our proposed Power-PLSTM model. Using ten different input combinations, the PLSTM model demonstrated superior predictive accuracy and lower error rates—especially with the Hi-Di-To input combination. It consistently outperformed traditional ML models such as LR and XGBoost, as well as other DL architectures including ANN, GRU, LSTM-ANN, and LSTM-RNN. These findings suggest that the PLSTM model can serve as a valuable tool for precise climate prediction in smart greenhouse systems. Importantly, the PLSTM model has already demonstrated its robustness on greenhouse databases from Mexico and Spain, where it was compared with ML models, and later with the Spain database to assess its performance against other DL models. It has also recently been applied to Moroccan greenhouse database, which is currently under submission. The deployment of PLSTM in real-world smart agriculture settings has the potential to significantly improve crop yield and resource efficiency by enabling timely and accurate climate control. Moreover, the model's adaptability to diverse greenhouse contexts highlights its scalability and potential for

global application. As the next step, we plan to integrate the model into our experimental greenhouse under construction in Morocco, where it will be deployed on an IoT platform for real-time environmental monitoring and control.

FUNDING INFORMATION

The authors would like to thank the Moroccan Ministry of Higher Education, Scientific Research and Innovation and the OCP Foundation who funded this work through the APRD research program. No specific grant number was assigned to this funding.

AUTHOR CONTRIBUTIONS STATEMENT

This journal uses the Contributor Roles Taxonomy (CRediT) to recognize individual author contributions, reduce authorship disputes, and facilitate collaboration.

Name of Author	C	M	So	Va	Fo	I	R	D	O	E	Vi	Su	P	Fu
Salma Ait Oussous	✓	✓	✓	✓	✓	✓		✓	✓	✓	✓			
Dauris Lail Madama		✓	✓					✓	✓		✓			
Rachid El Bouayadi	✓		✓	✓		✓			✓		✓		✓	
Aouatif Amine	✓	✓		✓	✓		✓			✓	✓	✓		✓

C : **C**onceptualization
M : **M**ethodology
So : **So**ftware
Va : **Va**lidation
Fo : **Fo**rmal Analysis
I : **I**nvestigation
R : **R**esources
D : **D**ata Curation
O : Writing - **O**riginal Draft
E : Writing - Review & **E**diting
Vi : **Vi**sualization
Su : **Su**pervision
P : **P**roject Administration
Fu : **Fu**nding Acquisition

CONFLICT OF INTEREST STATEMENT

Authors state no conflict of interest.

DATA AVAILABILITY

The data supporting the findings of this study are available from the corresponding author upon reasonable request.

REFERENCES

[1] R. De Witte, D. Janssen, S. S. Gmada, and C. García-García, "Best practices for training in sustainable greenhouse horticulture," *Sustainability*, vol. 15, no. 7, p. 5816, 2023, doi: 10.3390/su15075816.

[2] F. Mahmood, R. Govindan, A. Bermak, D. Yang, and T. Al-Ansari, "Data-driven robust model predictive control for greenhouse temperature control and energy utilisation assessment," *Applied Energy*, vol. 343, p. 121190, 2023, doi: 10.1016/j.apenergy.2023.121190.

[3] S. A. Oussous, D. L. Madama, A. Amine, and R. El Bouayadi, "Enhanced Predictive Modeling of Greenhouse Temperature Using Power Long Short Term Memory (PLSTM) model," in *2024 4th International Conference on Electrical, Computer, Communications and Mechatronics Engineering (ICECCME)*, Male, Maldives, 2024, pp. 1-6, doi: 10.1109/ICECCME62383.2024.10796211.

[4] S. M. Gharghory, "Deep network based on long-short-term memory for time series prediction of microclimate data inside the greenhouse," *International Journal of Computational Intelligence and Applications*, vol. 19, no. 2, p. 2050013, 2020, doi: 10.1142/S146902682050013X.

[5] F. M. Shiri, T. Perumal, N. Mustapha, and R. Mohamed, "A comprehensive overview and comparative analysis on deep learning models: CNN, RNN, LSTM, GRU," *arXiv preprint*, 2023, doi: 10.48550/arXiv.2305.17473.

[6] S. M. N. Islam, N. Thakur, K. Garg, and A. Gupta, "A recent survey on LSTM techniques for time-series data forecasting: Present state and future directions," in *Applications of Artificial Intelligence, Big Data and Internet of Things in Sustainable Development*, CRC Press, 2022, pp. 123–132, doi: 10.1201/9781003245469-8.

[7] A. Asllam, L. Lahoucine, A. A. Bari, and M. Amzil, "Moroccan and Spanish agriculture comparative analysis 2008–2021," in *Agriculture and Food Sciences Research*, vol. 11, no. 1, pp. 1–14, 2024, doi:10.20448/aesr.v11i1.5261.

[8] J. Janick, "Horticulture in Morocco: North Africa's California," in *HortScience*, vol. 24, no. 1, pp. 18–22, 1989.

[9] M. Eltehiwy and A. A. Abdul-Motaal, "A new method for computing and testing the significance of the Spearman rank correlation," *Computational Journal of Mathematical and Statistical Sciences*, vol. 2, no. 2, pp. 240–250, 2023, doi: 10.21608/cjmss.2023.229746.1015.

[10] J. Xia and Q. Shen, "Correlation analysis of different vegetable categories based on Spearman rank correlation coefficient," in *2024 IEEE 6th Advanced Information Management, Communicates, Electronic and Automation Control Conference (IMCEC)*, vol. 6, pp. 548–551, 2024, doi: 10.1109/IMCEC59810.2024.10575437.
[11] B. Bischl *et al.*, "Hyperparameter optimization: Foundations, algorithms, best practices, and open challenges," *Wiley Interdisciplinary Reviews: Data Mining and Knowledge Discovery*, vol. 13, no. 2, p. e1484, 2023, doi: 10.1002/widm.1484.
[12] S.-H. Han, H. Mutahira, and H.-S. Jang, "Prediction of sensor data in a greenhouse for cultivation of paprika plants using a stacking ensemble for smart farms," *Applied Sciences*, vol. 13, no. 18, p. 10464, 2023, doi: 10.3390/app131810464.
[13] Q. He, P. Shah, and X. Zhao, "Resilient operation of DC microgrid against FDI attack: A GRU based framework," *International Journal of Electrical Power and Energy Systems*, vol. 145, p. 108586, 2023, doi: 10.1016/j.ijepes.2022.108586.
[14] A. Kurani, P. Doshi, A. Vakharia, and M. Shah, "A comprehensive comparative study of artificial neural network (ANN) and support vector machines (SVM) on stock forecasting," *Annals of Data Science*, vol. 10, no. 1, pp. 183–208, 2023, doi: 10.1007/s40745-021-00344-x.
[15] A. T. Hoang *et al.*, "A review on application of artificial neural network (ANN) for performance and emission characteristics of diesel engine fueled with biodiesel-based fuels," *Sustainable Energy Technologies and Assessments*, vol. 47, p. 101416, 2021, doi: 10.1016/j.seta.2021.101416.
[16] Y. Chen, L. Song, Y. Liu, L. Yang, and D. Li, "A review of the artificial neural network models for water quality prediction," *Applied Sciences*, vol. 10, no. 17, p. 5776, 2020, doi: 10.3390/app10175776.
[17] T. Petrakis, A. Kavga, V. Thomopoulos, and A. A. Argiriou, "Neural network model for greenhouse microclimate predictions," *Agriculture*, vol. 12, no. 6, p. 780, May 2022, doi: 10.3390/agriculture12060780.
[18] Y. Qiu, T. Vo, D. Garg, H. Lee, and C. R. Kharangate, "A systematic approach to optimization of ANN model parameters to predict flow boiling heat transfer coefficient in mini/micro-channel heatsinks," *International Journal of Heat and Mass Transfer*, vol. 202, p. 123728, 2023, doi: 10.1016/j.ijheatmasstransfer.2022.123728.
[19] A. I. Lawal, "An artificial neural network-based mathematical model for the prediction of blast-induced ground vibration in granite quarries in Ibadan, Oyo State, Nigeria," *Scientific African*, vol. 8, p. e00413, 2020, doi: 10.1016/j.sciaf.2020.e00413.
[20] F. Kosanoglu, "Wind speed forecasting with a clustering-based deep learning model," *Applied Sciences*, vol. 12, no. 24, p. 13031, Dec. 2022, doi: 10.3390/app122413031.
[21] X. Yang and Z. Zhang, "A CNN-LSTM model based on a meta-learning algorithm to predict groundwater level in the middle and lower reaches of the Heihe River, China," *Water*, vol. 14, no. 15, p. 2377, Jul. 2022, doi: 10.3390/w14152377.
[22] N. F. Ali and M. Atef, "An efficient hybrid LSTM-ANN joint classification-regression model for PPG based blood pressure monitoring," *Biomedical Signal Processing and Control*, vol. 84, p. 104782, 2023, doi: 10.1016/j.bspc.2023.104782.
[23] X. Zhou, X. Meng, and Z. Li, "ANN-LSTM: A water consumption prediction based on attention mechanism enhancement," *Energies*, vol. 17, no. 5, p. 1102, 2024, doi: 10.3390/en17051102.
[24] P. Shah, H.-K. Choi, and J. S.-I. Kwon, "Achieving optimal paper properties: A layered multiscale kMC and LSTM-ANN-based control approach for kraft pulping," *Processes*, vol. 11, no. 3, p. 809, 2023, doi: 10.3390/pr11030809.
[25] J. Ge *et al.*, "Prediction of greenhouse tomato crop evapotranspiration using XGBoost machine learning model," *Plants*, vol. 11, no. 15, p. 1923, Jul. 2022, doi: 10.3390/plants11151923.
[26] R. Zhu, Y. Yang, and J. Chen, "XGBoost and CNN-LSTM hybrid model with attention-based stock prediction," in *2023 IEEE 3rd International Conference on Electronic Technology, Communication and Information (ICETCI)*, 2023, pp. 359–365, doi: 10.1109/ICETCI57876.2023.10176988.

BIOGRAPHIES OF AUTHORS

Salma Ait Oussous graduated with a Master's degree in Information Systems Security Research at the National School of Applied Sciences, Ibn Tofail University. She is currently pursuing her Ph.D. in the Advanced System Engineering Laboratory at the National School of Applied Sciences. Her research interests include artificial intelligence, internet of things (IoT) and their application in intelligent greenhouse systems. She can be contacted at email: salma.aitoussous@uit.ac.ma.

Dauris Lail Madama received his High School Diploma from Etat Jean Stanislas Migolet in Gabon. In 2020, he obtained a Higher Technician Diploma in Networks and Telecommunications from the National Institute of Posts, Information Technology, and Communications (INPTIC) in Gabon. Following that, he completed a bachelor's degree in networks and telecommunications, specializing in network administration and security, at INPTIC. Most recently, he earned a Master's degree in Information Systems Security from the National School of Applied Sciences (ENSA) in Kénitra, Morocco. He can be contacted at email: madamadauris95@gmail.com.

Prof. Rachid El Bouayadi is a Professor of materials science, specializing in ”surface and interface” studies, at the National School of Applied Sciences (ENSA) of Ibn Tofail University in Kenitra, Morocco. He heads the Department of Electrical Engineering, Telecommunications Networks, and Systems. In 2003, he earned his doctoral degree from Paul Cézanne University in France, with a thesis on the interaction between metallic impurities and cavities generated by high-energy helium implantation in a single silicon crystal. His research interests include transition metals, helium, crystalline silicon, and interstitial impurities, focusing on the behaviour and interactions of these materials at the microscopic level. He can be contacted at email: rachid.elbouayadi@uit.ac.ma.

Prof. Aouatif Amine is a Full Professor at the National School of Applied Sciences (ENSA) of Ibn Tofail University since 2010. In addition to her role at Ibn Tofail University, she has held invited positions at institutions like INSA de Rouen (France, 2017), UQAM (Canada, 2016) and the Johann Radon Institute(Austria, 2014). She also participated in the first Arab-American Frontiers Symposium at the Kuwait Institute for Scientific Research (Kuwait, 2011). She is widely recognized as a leading researcher in machine learning, deep learning, road safety using driver hypovigilance - pedestrian tracking, computer vision, and artificial intelligence. In addition, she is affiliated with organizations such as the IEEE Morocco Section, IEEE Computer Society, and the Association for Computing Machinery. She can be contacted at email: aouatif.amine@uit.ac.ma.